Diagnostic and Interventional Imaging (2019) **100**, 411—419

ORIGINAL ARTICLE /*Neuroradiology*

Predicting TERT promoter mutation using MR images in patients with wild-type IDH1 glioblastoma

K. Yamashita[a,*], **R. Hatae**[b], **A. Hiwatashi**[a], **O. Togao**[a], **K. Kikuchi**[a], **D. Momosaka**[a], **Y. Yamashita**[c], **D. Kuga**[b], **N. Hata**[b], **K. Yoshimoto**[b], **S.O. Suzuki**[d], **T. Iwaki**[d], **K. Iihara**[b], **H. Honda**[a]

[a] *Department of Clinical Radiology, Graduate School of Medical Sciences, Kyushu University, 812-8582 Fukuoka, Japan*
[b] *Department of Neurosurgery, Graduate School of Medical Sciences, Kyushu University, 812-8582 Fukuoka, Japan*
[c] *Department of Medical Technology, Kyushu University Hospital, 812-8582 Fukuoka, Japan*
[d] *Department of Neuropathology, Graduate School of Medical Sciences, Kyushu University, 812-8582 Fukuoka, Japan*

KEYWORDS
Magnetic resonance imaging (MRI);
Glioblastoma;
Telomerase reverse transcriptase (TERT);
Isocitrate dehydrogenase;
Support vector machine

Abstract
Purpose: The purpose of this study was to identify magnetic resonance imaging (MRI) features that are associated with telomerase reverse transcriptase promoter mutation (TERTm) in glioblastoma.
Materials and methods: A total of 112 patients with glioblastoma who had MRI at 1.5- or 3.0-T were retrospectively included. There were 43 patients with glioblastoma with wild-type TERT (TERTw) (22 men, 21 women; mean age, 47 ± 25 [SD] years; age range: 3—84 years) and 69 patients with glioblastoma with TERTm (34 men, 35 women; mean age 64 ± 11 [SD] years; age range, 41-—85 years). The feature vectors consist of 11 input units for two clinical parameters (age and gender) and nine MRI characteristics (tumor location, subventricular extension, cortical extension, multiplicity, enhancing volume, necrosis volume, the percentage of necrosis volume, minimum apparent diffusion coefficient [ADC] and normalized ADC). First, the diagnostic performance using univariate and multivariate logistic regression analyses was evaluated. Second, the cross-validation of the support vector machine (SVM) was performed by using leave-one-out method with 43 TERTw and 69 TERTm to evaluate the diagnostic performance. In addition, the sensitivity, specificity, positive predictive value (PPV), negative predictive value (NPV), and accuracy for the differentiation between TERTw and TERTm were compared between logistic regression analysis and SVM.

* Corresponding author.
E-mail address: yamakou@radiol.med.kyushu-u.ac.jp(K. Yamashita).

https://doi.org/10.1016/j.diii.2019.02.010

Results: With multivariate analysis, the percentage of necrosis volume and age were significantly greater in TERTm glioblastoma than in TERTw glioblastoma. SVM allowed discriminating between TERTw glioblastoma and TERTm glioblastoma with sensitivity, specificity, PPV, NPV, and accuracy of 85.7% [60/70; 95% confidence interval (CI): 75.3—92.9%], 54.8% (23/42; 95% CI: 38.7—70.2%), 75.9% (60/79; 95% CI: 69.1—81.7%), 69.7% (23/33; 95% CI: 54.9—81.3%) and 74.1% (83/112; 95% CI: 65.0—81.9%), respectively.
Conclusion: The percentage of necrosis volume and age may surrogate for predicting TERT mutation status in glioblastoma.

Glioblastoma is the most common type of primary high-grade brain tumor in adults [1]. The characteristic histological appearance of glioblastoma includes: hypercellularity, nuclear polymorphism, high mitotic activity, prominent microvascular proliferation and/or necrosis [2]. Conventional magnetic resonance imaging (MRI) techniques including pre- and post-contrast T1-weighted images show precise anatomical location and/or centrally non-enhancing areas, which are typically related histologically to necrotic areas. Diehn et al. have reported that the amount of necrosis is correlated with the outcome in patients with glioblastoma [3]. In addition, good correlations have been reported between the apparent diffusion coefficient (ADC) derived from diffusion-weight imaging and tumor cellularity and the utility of ADC in glioma grading has been addressed in several studies [4—8].

Genetic profiling may provide new insights into neuro-oncology. Telomerase reverse transcriptase (TERT) promoter mutations are frequently found in many types of human cancers and are associated with enhanced telomere maintenance [9,10]. The prevalence of TERT promoter mutations is remarkably high in adult glioblastoma [9,11,12]. Moreover, the combination of TERT promoter mutation and wild-type isocitrate dehydrogenase 1 (IDH1) is the most common genotype observed in glioblastoma [13]. Previous reports have shown that glioma patients with unmethylated O^6-methylguanine-DNA methyltransferase (MGMT) and TERT promoter mutation have worse prognosis than those with wild-type TERT [13,14]. Therefore, preoperative detection of TERT promoter mutation would be of great importance to patients with glioblastoma and may impact therapeutic strategies such as telomerase-targeted therapies [15,16].

The purpose of this study was to identify MRI features that are associated with TERT promoter mutation in glioblastoma.

Materials and methods

This study was approved by the Kyushu University institutional review board for clinical research. Informed consent for study participation was waived due to the retrospective nature of this study.

Patients

MRI data for consecutive patients from January 2003 to May 2016 were obtained and retrospectively analyzed. There was a total of 139 patients who underwent preoperative MRI with histologically proven glioblastoma and obtained TERT promoter mutation status. Patients with recurrent tumors and mutant IDH glioblastoma were excluded.

The study population consisted of 43 patients with glioblastoma with wild-type TERT (TERTw) [22 men, 21 women; mean age, 47 ± 25 (SD) years; age range, 3—84 years] and 69 patients with glioblastoma with *TERT* promoter mutation (TERTm) [34 men, 35 women; mean age, 64 ± 11(SD); age range, 41—85 years]. Fig. 1 shows the flow chart diagram. All glioblastomas were surgically resected and the diagnosis was made histopathologically by experienced neuropathologists. The mean time interval between MRI examination and surgery was 6.9 days (range: 0—21 days).

MRI protocol

The MRI examination were obtained using at 1.5-T (Magnetom Vision® or Symphony®, Siemens Healthineers) or 3.0-T (Achieva® or Ingenia®, Philips Healthcare). Pre- and post-contrast T1-weighted spin echo images were obtained in the transverse plane. The acquisition parameters are listed in Table 1. A standard dose (0.1 mmol/kg body weight) of a gadolinium-based contrast agent (gadopentetate dimeglumine, Magnevist®, Bayer Healthcare), gadoteridol (ProHance®, Eisai), or gadodiamide (Omniscan®, Daiichi Sankyo), was injected intravenously.

Diffusion-weighted imaging was performed using a single-shot spin echo-planar sequence. The acquisition parameters are listed in Table 1. Diffusion sensitizing gradients were applied sequentially in the *x*, *y*, and *z* directions with *b* factors of 0 and 1000 s/mm^2.

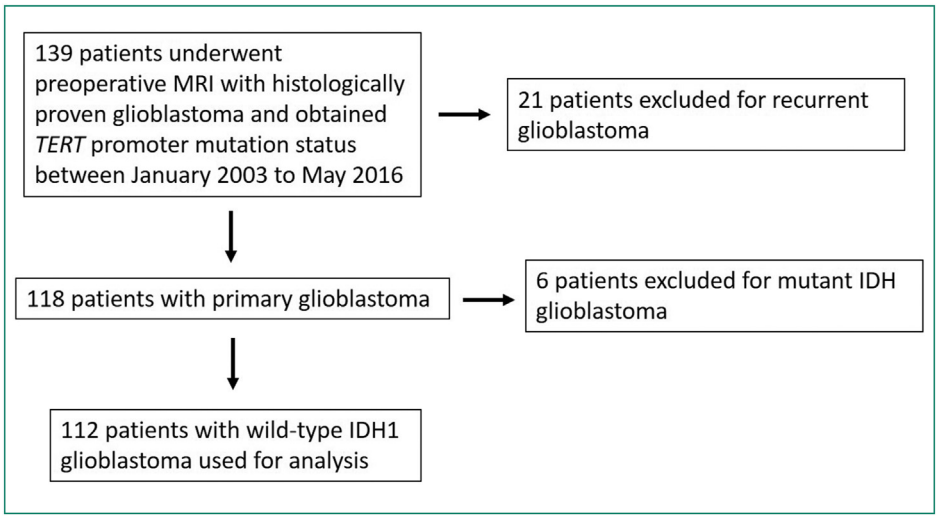

Figure 1. Flow chart shows patients inclusion into the study.

Table 1 Magnetic resonance imaging protocol.

	1.5-Teslanewline Vision® (*N* = 16)	Symphony® (*N* = 8)	3.0-Teslanewline Achieva® (*N* = 79)	Ingenia® (*N* = 9)
Pre-contrast T1-weighted MRI				
TR/TE (ms)	493—551/11—14	493—494/11	400—424/10	450—452/8.7—9
FA (°)	90	80	90	75
Matrix	512 × 192	256 × 192—208	256 × 217	256 × 205
FOV	230 × 230	172.5—230 × 230	230 × 230	230 × 230
Slice thickness/gap (mm)	5/2.5	5/2.5	5/1	5/1
Post-contrast T1-weighted MRI				
TR/TE (msec)	541—636/17	541—624/17	400—498/17—20	440—480/21
FA (°)	90	80	90	75
Matrix	512 × 192	256 × 192—208	256 × 217	256 × 205
FOV	230 × 230	172.5—230 × 230	230 × 230	230 × 230
Slice thickness/gap (mm)	5/2.5	5/2.5	5/1	5/1
Diffusion-weighted MRI				
TR/TE (msec)	2487/137	3100—3400/119	3421—4000/62—72	4094—4504/68—7
FA (°)	90	90	90	90
Matrix	128 × 128	200 × 96	160 × 127	160 × 126
FOV	230 × 230	230 × 230	230 × 230	230 × 230
Slice thickness/gap (mm)	5/2.5	5/2.5	5/1	5/1

Detection of IDH1 and TERT mutations in glioblastoma tissues

The method for detection of IDH1 mutations has been described in detail elsewhere [17]. PCR and sequencing of the TERT promoter were performed according to a previous study [18]. We designed the required oligonucleotide primers by using Primer3Plus: forward primer TERTf 5′-GGCCGATTCGACCTCTCT-3′ and the antisense primer TERTf 5′-CAGCGCTGCCTGAAACTC-3′. PCR was performed in a 10-μL reaction volume containing approximately 20 ng of genomic DNA, 0.1 μL of TaKaRa LA Taq (TaKaRa Bio Inc., Kusatsu, Japan), 5 μL of 2 × GC Buffer I, 1.6 μL of a dNTP mixture (2.5 mM each), and 1.67 μL of each primer (2 μM). The PCR conditions were as follows: initial denaturation at 95 °C for 5 min, followed by 35 cycles of 94 °C for 30 s, 62 °C for 30 s, and 72 °C for 30 s, and a final elongation at 72 °C for 7 min. PCR products were purified using ExoSAP-IT (Affymetrix/USB), after which cycle sequencing was performed using BigDye® Terminator v3.1 Cycle Sequencing Kits (Applied Biosystems). Following purification, electrophoresis and analysis were conducted using a PRISM® 310 Genetic Analyzer (Applied Biosystems).

MR image evaluation

For each glioblastoma, the enhancing volume on post-contrast T1-weighted images was calculated manually and multiplied by the MRI section thickness. Pre-contrast T1-weighted images were used as references. Necrosis and the

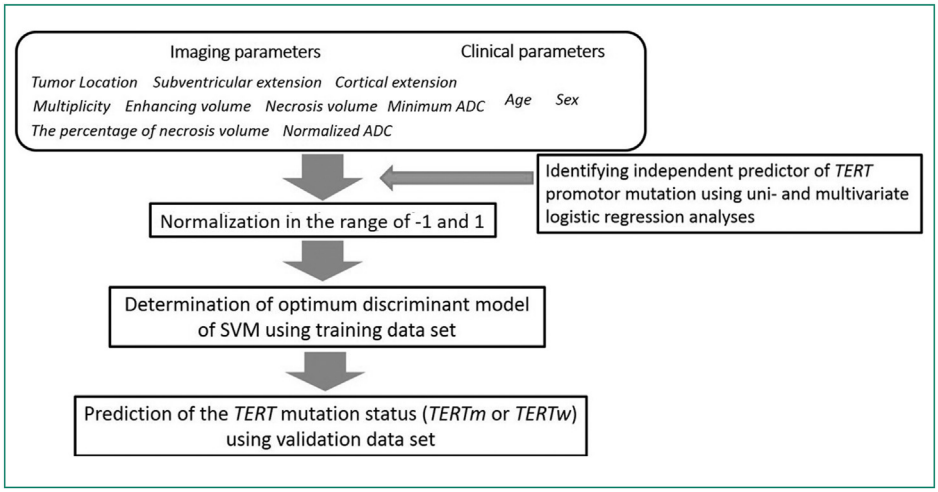

Figure 2. Steps for classification using a support vector machine.

percentage of necrosis volume were determined by measuring the non-enhancing area within the maximum enhancing lesion, which were manually outlined on each slice. The measurement of ADC value was performed using region of interest (ROI) analysis. Three ROIs were placed in the enhancing lesion more than 10 mm^2 each. Regions with relatively low ADC were targeted, while careful attention was paid to avoid contamination of blood vessels, calcification, necrosis, and hemorrhage for ROI placement. The average ADC values chosen from three ROIs were determined as the minimum ADC (ADC_{min}) [19]. In addition, large circular ROI (> 100 mm^2) was placed in contralateral normal appearing white matter (NAWM). To reduce the variations among images acquired on the different scanners, ADC_{min} values were normalized to the contralateral NAWM. Normalized ADC (nADC) was determined the ratio between ADC_{min} and ADC values in NAWM [20]. For tumor enhancement, the multiple type was defined as a tumor with at least two distinct foci such as multifocal or dissemination [21]. Unifocal enhancing tumors were considered solitary glioblastoma. When multifocal lesions were noted, the histopathologically assessed lesion was measured. These determinations were performed by the first author (K.Y., with 16 years of experience in neuroradiology), followed by visual inspection by another neuroradiologist (O.T., with 18 years of experience in neuroradiology). The observers were blinded to the TERT mutation status.

Glioblastoma location was divided into seven regions: frontal, parietal, temporal, occipital lobes, insular region, basal nuclei or thalamus, and brainstem or cerebellum. The location was determined as the main area of glioblastoma involvement and was visually identified by a neuroradiologist (K.Y., with 16 years of experience in neuroradiology).

Construction of support vector machine

We constructed a support vector machine (SVM) classifier with a Gaussian kernel by using the free commercial software (SVM^{light} version 6.0.2, http://svmlight joachims.org/). The feature vectors consisted of 11 input units for two clinical parameters (age and gender) and nine MRI characteristics (tumor location, subventricular extension, cortical extension, multiplicity, enhancing volume, necrosis volume, the percentage of necrosis volume, ADC_{min}, and nADC) (Fig. 2). All input parameters were normalized to a value in the range of −1.0 to 1.0. Second, non-linear transformation with Gaussian kernel function was performed. Then, the cross-validation of the SVM was performed by using leave-one-out method with 43 TERTw and 69 TERTm to evaluate the diagnostic performance.

Statistical analysis

First, the value of each parameter was compared between TERTm and TERTw using univariate logistic regression and multivariate logistic regression analyses. Pearson's chi-square test was applied to evaluate the different categories for tumor location. Second, using independent predictors of TERT promoter mutation based on the univariate logistic regression analysis, the sensitivity, specificity, positive predictive value (PPV), negative predictive value (NPV), and accuracy for the differentiation between TERTw and TERTm were compared between logistic regression analysis and SVM using a nonparametric approach. The area under the curve (AUC) values obtained from SVM and logistic regression analysis were compared. A P value < 0.05 was considered to indicate statistical significance for univariate logistic regression and multivariate logistic regression

Table 2 Location of glioblastoma.

	TERTw (N = 43)	TERTm (N = 69)
Frontal lobe	15 (34.9)	21 (30.4)
Parietal lobe	7 (16.3)	18 (26.1)
Temporal lobe	5 (11.6)	16 (23.2)
Occipital lobe	0 (0.0)	3 (4.3)
Insula	2 (4.7)	5 (7.2)
Basal nuclei or thalamus	10 (23.3)	6 (8.7)
Brainstem or cerebellum	4 (9.3)	0 (0.0)

Numbers are raw numbers followed by percentages in parenthesis.

analyses. All statistical analyses except for the SVM were performed using JMP 11 Pro software (SAS Institute, Cary).

Results

The enhancing volume, necrosis volume, and percentage of necrosis volume were significantly greater in patients with TERTm [mean enhancing volume = 39.9 ± 34.8 (SD) $\times 10^3$ mm^3 (range: 1.2—179.5×10^3 mm^3); mean necrosis volume = 17.5 ± 16.8 (SD) $\times 10^3$ mm^3 (range: 0—80.1×10^3 mm^3); and mean percentage of necrosis volume = 39.4 ± 17.8 (SD) % (range: 0—77.4%)] than in those with TERTw [mean enhancing volume = 24.8 ± 21.4 (SD) $\times 10^3$ mm^3 (range: 0.2—80.6×10^3 mm^3), mean necrosis volume = 8.6 ± 10.3 (SD) $\times 10^3$ mm^3 (range: 0—40.7×10^3 mm^3), and mean percentage of necrosis volume = 26.7 ± 19.2 (SD) % (range: 0—67.0%) ($P < 0.0129$, 0.0016, and 0.0012, respectively)]. No differences were found in ADC_{min} [$ADC_{min} = 0.8 \pm 0.6$ (SD) $\times 10^{-3}$ mm^2/s; range: 0.7—1.1×10^{-3} mm^2/s in TERTm, 0.8 ± 0.7 (SD) $\times 10^{-3}$ mm^2/s; range, 0.7—0.9×10^{-3} mm^2/s in TERTw] and nADC [nADC = 1.2 ± 0.3 (SD) $\times 10^{-3}$ mm^2/s; range, 0.7—2.0 in TERTm, 1.1 ± 0.3 (SD) $\times 10^{-3}$ mm^2/s; range, 0.7—1.8 in TERTw, ($P = 0.9451$ and 0.2965, respectively)].

Univariate analysis showed that age, glioblastoma location, cortical extension, enhancing volume, necrosis volume, and percentage of necrosis volume were independent predictors of TERT promoter mutation (Tables 2 and 3). Multivariate analysis showed that age and percentage of necrosis volume were significantly greater in TERTm glioblastoma than in TERTw glioblastoma (Table 3).

SVM using leave-one out method allowed differentiation between TERTw and TERTm with sensitivity, specificity, PPV, NPV, and accuracy of 85.7% [60/70; 95% confidence interval (CI): 75.3—92.9%], 54.8% (23/42; 95% CI = 38.7—70.2%), 75.9% (60/79; 95% CI: 69.1—81.7%), 69.7% (23/33; 95% CI: 54.9—81.3%) and 74.1% (83/112; 95% CI: 65.0—81.9%), respectively (Table 4). The AUC values obtained from SVM and logistic regression analysis were 0.776 and 0.776, respectively. No differences in AUC values were found between SVM and logistic regression analysis. Figs. 3 and 4 show representative patients with TERTm and TERTw gliobastoma, respectively.

Discussion

In this study, we found that the percentage of necrosis was greater in TERTm than in TERTw. Previous studies have shown that TERT promoter mutation increases the levels of epidermal growth factor receptor amplification and interleukin 6, which induces tumor angiogenesis and necrosis [9,12,22]. Epidermal growth factor receptor amplification, a classic molecular feature of primary glioblastoma, exclu-

Table 3 Results of univariate and multi-variate logistic regression analyses.

	TERTw ($N = 43$)	TERTm ($N = 69$)	P (univariate)	P (multi-variate)
Tumor location			0.0155	0.2719
Subventricular extension	39.5% (17/43)	40.6% (28/69)	0.9127	
Cortical extension	34.9% (15/43)	58.0% (40/69)	0.0175	0.2021
Multiplicity	32.6% (14/43)	49.3% (34/69)	0.0821	
Enhancing volume ($\times 10^3$ mm^3)	24.8 ± 21.4 [0.2—80.6]	39.9 ± 34.8 [1.2—179.5]	0.0129	0.8536
Necrosis volume ($\times 10^3$ mm^3)	8.6 ± 10.3 [0—40.7]	17.5 ± 16.8 [0—80.1]	0.0016	0.4228
Percentage of necrosis volume (%)	26.7 ± 19.2 [0—67.0]	39.4 ± 17.8 [0—77.4]	0.0012	0.0268
Minimum ADC ($\times 10^{-3}$ mm^2/s)	0.8 ± 0.7 [0.7—0.9]	0.8 ± 0.6 [0.7—1.1]	0.9451	
Normalized ADC ($\times 10^{-3}$ mm^2/s)	1.1 ± 0.3 [0.7—1.8]	1.2 ± 0.3 [0.7—2.0]	0.2965	
Age (years)	47 ± 25 [3—84]	64 ± 11 [41—85]	0.0003	0.0127
Sex (M/F)	22/21	34/35	0.8459	

ADC indicates apparent diffusion coefficient. Quantitative variables are expressed as mean ± standard deviation, followed by ranges in brackets. Qualitative variables are expressed as percentages (%) followed by proportions in parentheses.

Table 4 Sensitivity, specificity, and accuracy for the differentiation between patients with TERT promoter mutation and wild-type TERT glioblastoma.

	SVM (leave-one-out method)	Logistic regression analysis ($N = 112$)
Sensitivity	85.7% (60/70) [75.3—92.9%]	97.1% (67/69) [89.9—99.7%]
Specificity	54.8% (23/42) [38.7—70.2%]	46.5% (20/43) [31.2—62.4%]
PPV	75.9% (60/79) [69.1—81.7%]	74.4% (67/90) [68.7—79.4%]
NPV	69.7% (23/33) [54.9—81.3%]	90.9% (20/22) [71.1—97.6%]
Accuracy	74.1% (83/112) [65.0—81.9%]	77.7% (87/112) [68.8—85.0%]
AUC	0.776	0.776

The numbers in parenthesis are proportions; Numbers in brackets are 95% confidence intervals; SVM indicates support vector machine. PPV indicates positive predictive value. NPV indicates negative predictive value.

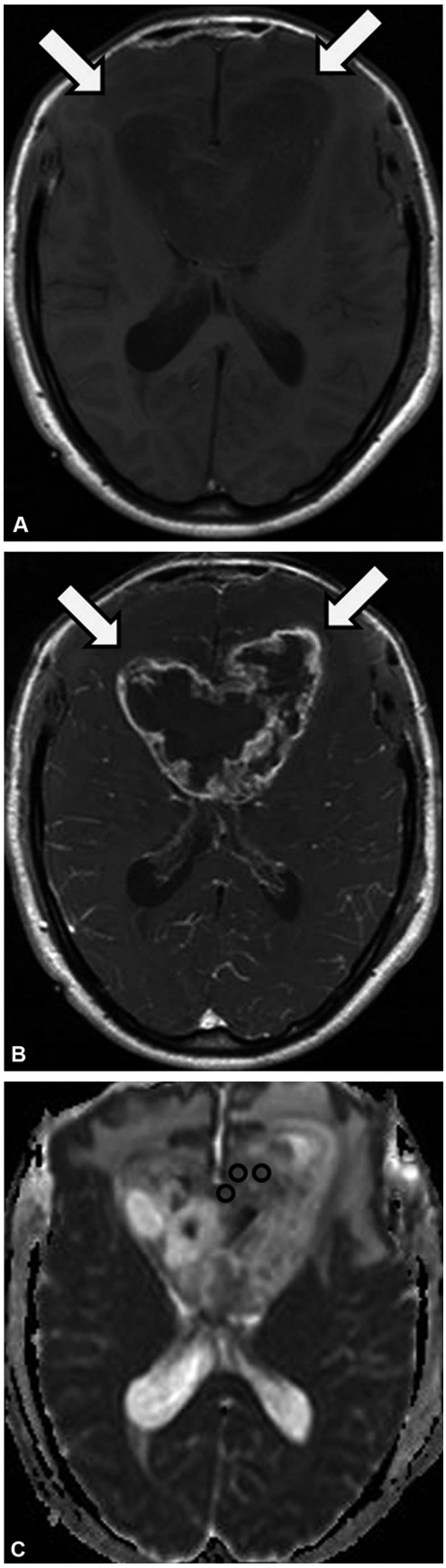

Figure 3. 41-year-old woman with glioblastoma with telomerase reverse transcriptase promoter mutation who underwent MRI at 3 Tesla. A: T1-weighted MR image obtained in the axial plane before intravenous administration of a gadolinium chelate and; B: T1-weighted MR image obtained in the axial plane after intravenous administration of a gadolinium chelate show glioblastoma (arrows); C: Apparent diffusion coefficient (ADC) map derived from diffusion-weighted image. Three circular regions of interest (black circles) were placed in the lesion that displays relatively high enhancing volume ($28.2 \times 10^3\ mm^3$) and high percentage of necrosis volume (70.9%). The ADC_{min} value is $1.208 \times 10^{-3}\ mm^2/s$.

sively occurred in tumors with TERTm [9]. In addition, Ahmad et al. revealed that glioblastoma patients with TERTm were associated with lower glycogen accumulation [23]. The decreased glycogen breakdown induces cancer cell apoptosis by limiting glucose oxidation, as well as nucleic acid and de novo fatty acid synthesis. These results suggested that necrosis may be more frequent in patients with TERT promoter mutation.

Previous studies have shown that glioma patients with TERT promoter mutation are significantly older than those with wild-type TERT, and glioma prognosis is related to age at diagnosis [10,11]. In addition, TERT promoter mutation is common in patients older than 55 years [24]. Therefore, age could have some influence on TERT mutation frequency. Our results are in line with the literature.

Glioblastoma location may be used as a predictor of TERT promoter mutation status. Previous studies showed that TERTm gliomas are more likely to be located in the frontal [25] or temporal lobe [26]. In the present study, univariate logistic regression analysis indicated that glioblastoma location was one of the independent predictors of TERT promoter mutation, whereas multivariate logistic regression revealed no significant differences between TERTw and TERTm. These results suggested that the basal nuclei/thalamus and brainstem/cerebellum might be associated with wild-type TERT promoter in glioblastoma. Further validation study is needed.

We observed no associations between TERT promoter mutation and subventricular extension. Simon et al. also revealed no correlation between TERT mutation and the presumed glioblastoma origin in the subventricular zone [27]. A different mechanism may operate in subventricular zone involvement and TERT promoter mutation.

No difference in ADC values were found between TERTw and TERTm glioblastomas with either SVM or logistic regression analysis in our study. Based on a radiologic-pathologic correlation study, no significant correlations between the Ki-67 labeling index and minimum ADC were noted for the glioblastoma group [4]. Our results are consistent with those of the literature.

In the present study, the SVM provided moderate accuracy for differentiating between TERTm and TERTw glioblastoma. SVM algorithms have been proven to constitute a good classifier and prediction method because the results were obtained using a training and validation cohort method [28]. SVM with leave-one-out method and logistic regression analysis using all subjects' data showed similar diagnostic accuracy for discriminating between TERTm and TERTw glioblastoma in our study. Compared to logistic regression, SVMs are designed to generate more complex

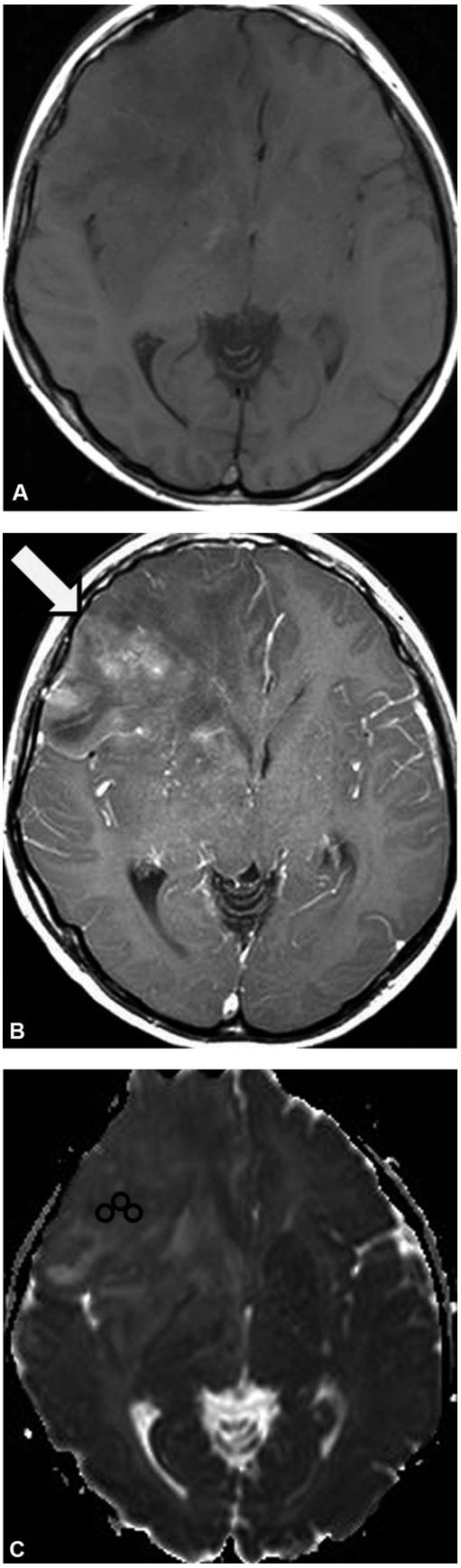

Figure 4. 26-year-old woman with glioblastoma with wild-type telomerase reverse transcriptase who underwent MRI at 3 Tesla. A: T1-weighted MR image obtained in the axial plane before intravenous administration of a gadolinium chelate and; B: T1-weighted MR image obtained in the axial plane after intravenous administration of a gadolinium chelate show glioblastoma (arrow); C: Apparent diffusion coefficient (ADC) map derived from diffusion-weighted image. Three circular regions of interest (black circles) were placed in the lesion that displays low enhancing volume (4.0×10^3 mm^3) and low percentage of necrosis volume (0.67%). The ADC_{min} value is 0.916×10^{-3} mm^2/s.

decision boundaries [29]. In addition, logistic regression analysis is an indirect method that maximizes the likelihood of data, whereas an SVM directly maximizes the margin between the two groups. TERT promoter mutation is influenced by many environmental factors [10,30]. The molecular basis of heterogeneity in gliomas was shown by early studies [31—34]. These results suggested that multiple factors are likely associated with genetic alterations. Taken together, an SVM using a multi-parametric approach may offer a more objective method and reinforce the results obtained from logistic regression analyses.

Our study has some limitations. First, 3D measurement data were not available and we used four different MRI scanners. Second, glioblastoma patients with IDH mutation should be included. However, the sample size was much smaller than patients with wild-type IDH1 glioblastoma. Third, both adult and pediatric patients were included in this study. It is known that pediatric and adult high-grade gliomas are biologically different [35]. We focused on the TERT promoter and IDH1 mutation status to reduce the potential of selection bias in the present study. Fourth, the extent of peritumoral edema reflects extracellular water and is useful for the differentiation between glioblastoma and solitary metastatic tumor [36]. Whereas, the ''peritumoral edema'' contains a mixture of both edema and cell invasion in glioblastoma [37]. The administration of steroid or antihydrophic agents makes it difficult to interpret the peritumoral white matter. Finally, perfusion-weighted MRI (such as arterial spin labeling, dynamic susceptibility contrast, or dynamic contrast enhanced imaging), and glioblastoma metabolic assessment using MR spectroscopy or positron emission tomography imaging were not available in the present study. We believe that the addition of these advanced imaging features will have a deeper understanding the angiogenesis status, hypoxia, and proliferation status of glioblastoma, or enhance SVM-based classification, and doing so is our next step.

In conclusion, the percentage of necrosis volume and age may surrogate for predicting TERT mutation status in patients with wild-type IDH1 glioblastoma.

Ethical approval

This study was approved by the institutional review board of our hospital (Kyushu University Institutional Review Board for Clinical Research).

Informed consent

Informed consent for study participation was waived due to the retrospective nature of this study.

Author contribution statements

K.Y. designed the model. K.Y. and O.T. carried out the implementation. K.Y. wrote the manuscript in consultation with A.H., T.I., K.I. and H.H. H.R., D.K., N.H., K.Y., S.O.S., and T.I. contributed to sample preparation. Y.Y. performed the analytic calculations and performed the numerical simulations. K.K. and D.M. aided in interpreting the results and worked on the manuscript. All authors discussed the results and commented on the manuscript. K.Y. and R.H. equally contributed to this work.

Funding

This work was supported by the Japan Society for the Promotion of Science (Grant Number 17K10365).

Disclosure of interest

The authors declare that they have no competing interest.

References

[1] Chamberlain MC, Kormanik PA. Practical guidelines for the treatment of malignant gliomas. West J Med 1998;168:114—20.
[2] Burger PC, Green SB. Patient age, histologic features, and length of survival in patients with glioblastoma multiforme. Cancer 1987;59:1617—25.
[3] Diehn M, Nardini C, Wang DS, McGovern S, Jayaraman M, Liang Y, et al. Identification of noninvasive imaging surrogates for brain tumor gene-expression modules. Proc Natl Acad Sci USA 2008;105:5213—8.
[4] Higano S, Yun X, Kumabe T, Watanabe M, Mugikura S, Umetsu A, et al. Malignant astrocytic tumors: clinical importance of apparent diffusion coefficient in prediction of grade and prognosis. Radiology 2006;241:839—46.
[5] Tien RD, Felsberg GJ, Friedman H, Brown M, MacFall J. MR imaging of high-grade cerebral gliomas: value of diffusion-weighted echoplanar pulse sequences. AJR Am J Roentgenol 1994;162:671—7.
[6] Provenzale JM, Mukundan S, Barboriak DP. Diffusion-weighted and perfusion MR imaging for brain tumor characterization and assessment of treatment response. Radiology 2006;239:632—49.
[7] Kono K, Inoue Y, Nakayama K, Shakudo M, Morino M, Ohata K, et al. The role of diffusion-weighted imaging in patients with brain tumors. Am J Neuroradiol 2001;22:1081—8.
[8] Cihangiroglu MM, Ozturk-Isik E, Firat Z, Kilickesmez O, Ulug AM, Ture U. Preoperative grading of supratentorial gliomas using high or standard b-value diffusion-weighted MR imaging at 3T. Diagn Interv Imaging 2017;98:261—8.
[9] Killela PJ, Reitman ZJ, Jiao Y, Bettegowda C, Agrawal N, Diaz LAJr, et al. TERT promoter mutations occur frequently in gliomas and a subset of tumors derived from cells with low rates of self-renewal. Proc Natl Acad Sci USA 2013;110:6021—6.
[10] Chen C, Han S, Meng L, Li Z, Zhang X, Wu A. TERT promoter mutations lead to high transcriptional activity under hypoxia and temozolomide treatment and predict poor prognosis in gliomas. PloS one 2014;9:e100297.
[11] Eckel-Passow JE, Lachance DH, Molinaro AM, Walsh KM, Decker PA, Sicotte H, et al. Glioma groups based on 1p/19q, IDH, and TERT promoter mutations in tumors. N Engl J Med 2015;372:2499—508.
[12] Nonoguchi N, Ohta T, Oh JE, Kim YH, Kleihues P, Ohgaki H. TERT promoter mutations in primary and secondary glioblastomas. Acta Neuropathol 2013;126:931—7.
[13] Arita H, Yamasaki K, Matsushita Y, Nakamura T, Shimokawa A, Takami H, et al. A combination of TERT promoter mutation and MGMT methylation status predicts clinically relevant subgroups of newly diagnosed glioblastomas. Acta Neuropathol Commun 2016;4:79.
[14] Nguyen HN, Lie A, Li T, Chowdhury R, Liu F, Ozer B, et al. promoter mutation enables survival advantage from MGMT promoter methylation in IDH1 wild-type primary glioblastoma treated by standard chemoradiotherapy. Neuro Oncol 2017;19:394—404.
[15] Arita H, Narita Y, Fukushima S, Tateishi K, Matsushita Y, Yoshida A, et al. Upregulating mutations in the TERT promoter commonly occur in adult malignant gliomas and are strongly associated with total 1p19q loss. Acta Neuropathol 2013;126:267—76.
[16] Ruden M, Puri N, Novel anticancer therapeutics targeting telomerase. Cancer Treat Rev 2013;39:444—56.
[17] Hatae R, Hata N, Yoshimoto K, Kuga D, Akagi Y, Murata H, et al. Precise detection of IDH1/2 and BRAF hotspot mutations in clinical glioma tissues by a differential calculus analysis of high-resolution melting data. PloS one 2016;11:e0160489.
[18] Hatae R, Hata N, Suzuki SO, Yoshimoto K, Kuga D, Murata H, et al. A comprehensive analysis identifies BRAF hotspot mutations associated with gliomas with peculiar epithelial morphology. Neuropathology 2017;37:191—9.
[19] Yamashita K, Hiwatashi A, Togao O, Kikuchi K, Hatae R, Yoshimoto K, et al. MR Imaging-based analysis of glioblastoma multiforme: estimation of IDH1 mutation status. AJNR Am J Neuroradiol 2016;37:58—65.
[20] Pierce TT, Provenzale JM. Evaluation of apparent diffusion coefficient thresholds for diagnosis of medulloblastoma using diffusion-weighted imaging. Neuroradiol J 2014;27:63—74.
[21] Patil CG, Yi A, Elramsisy A, Hu J, Mukherjee D, Irvin DK, et al. Prognosis of patients with multifocal glioblastoma: a case-control study. J Neurosurg 2012;117:705—11.
[22] Mosrati MA, Malmstrom A, Lysiak M, Krysztofiak A, Hallbeck M, Milos P, et al. TERT promoter mutations and polymorphisms as prognostic factors in primary glioblastoma. Oncotarget 2015;6:16663—73.
[23] Ahmad F, Dixit D, Sharma V, Kumar A, Joshi SD, Sarkar C, et al. Nrf2-driven TERT regulates pentose phosphate pathway in glioblastoma. Cell Death Dis 2016;7:e2213.
[24] Lee Y, Koh J, Kim SI, Won JK, Park CK, Choi SH, et al. The frequency and prognostic effect of TERT promoter mutation in diffuse gliomas. Acta Neuropathol Commun 2017;5:62.
[25] Sun ZL, Chan AK, Chen LC, Tang C, Zhang ZY, Ding XJ, et al. TERT promoter mutated WHO grades II and III gliomas are located preferentially in the frontal lobe and avoid the midline. Int J Clin Exp Pathol 2015;8:11485—94.
[26] Fan X, Wang Y, Liu Y, Liu X, Zhang C, Wang L, et al. Brain regions associated with telomerase reverse transcriptase promoter mutations in primary glioblastomas. J Neurooncol 2016;128:455—62.
[27] Simon M, Hosen I, Gousias K, Rachakonda S, Heidenreich B, Gessi M, et al. TERT promoter mutations: a novel

independent prognostic factor in primary glioblastomas. Neuro Oncol 2015;17:45—52.
[28] Verplancke T, Van Looy S, Benoit D, Vansteelandt S, Depuydt P, De Turck F, et al. Support vector machine versus logistic regression modeling for prediction of hospital mortality in critically ill patients with haematological malignancies. BMC Med Inform Decis Mak 2008;8:56.
[29] Pochet NL, Suykens JA. Support vector machines versus logistic regression: improving prospective performance in clinical decision-making. Ultrasound Obstet Gynecol 2006;27:607—8.
[30] Oliveira RP, Porter Abate J, Dilks K, Landis J, Ashraf J, Murphy CT, et al. Condition-adapted stress and longevity gene regulation by Caenorhabditis elegans SKN-1/Nrf. Aging cell 2009;8:524—41.
[31] Bonavia R, Inda MM, Cavenee WK, Furnari FB. Heterogeneity maintenance in glioblastoma: a social network. Cancer Res 2011;71:4055—60.
[32] Wikstrand CJ, Bigner SH, Bigner DD. Demonstration of complex antigenic heterogeneity in a human glioma cell line and eight derived clones by specific monoclonal antibodies. Cancer Res 1983;43:3327—34.
[33] Shapiro JR, Yung WK, Shapiro WR. Isolation, karyotype, and clonal growth of heterogeneous subpopulations of human malignant gliomas. Cancer Res 1981;41:2349—59.
[34] Parker NR, Khong P, Parkinson JF, Howell VM, Wheeler HR. Molecular heterogeneity in glioblastoma: potential clinical implications. Front Oncol 2015;5:55.
[35] Nishikawa R. Pediatric and adult gliomas: how different are they? Neuro Oncol 2010;12:1203—4.
[36] Lu S, Ahn D, Johnson G, Cha S. Peritumoral diffusion tensor imaging of high-grade gliomas and metastatic brain tumors. AJNR Am J Neuroradiol 2003;24:937—41.
[37] Zinn PO, Mahajan B, Sathyan P, Singh SK, Majumder S, Jolesz FA, et al. Radiogenomic mapping of edema/cellular invasion MRI-phenotypes in glioblastoma multiforme. PloS One 2011;6:e25451.